

# Power-law velocity distributions in granular gases

E. Ben-Naim,<sup>1,\*</sup> B. Machta,<sup>2,3,†</sup> and J. Machta<sup>3,‡</sup>

<sup>1</sup>*Theoretical Division and Center for Nonlinear Studies,*

*Los Alamos National Laboratory, Los Alamos, New Mexico 87545*

<sup>2</sup>*Department of Physics, Brown University, Providence, Rhode Island 02912*

<sup>3</sup>*Department of Physics, University of Massachusetts, Amherst, Massachusetts 01003*

We report a general class of steady and transient states of granular gases. We find that the kinetic theory of inelastic gases admits stationary solutions with a power-law velocity distribution,  $f(v) \sim v^{-\sigma}$ . The exponent  $\sigma$  is found analytically and depends on the spatial dimension, the degree of inelasticity, and the homogeneity degree of the collision rate. Driven steady-states, with the same power-law tail and a cut-off can be maintained by injecting energy at a large velocity scale, which then cascades to smaller velocities where it is dissipated. Associated with these steady-states are freely cooling time-dependent states for which the cut-off decreases and the velocity distribution is self-similar.

PACS numbers: 45.70.Mg, 47.70.Nd, 05.40.-a, 81.05.Rm

## I. INTRODUCTION

The statistical physics of granular gases is unusual in many ways [1, 2, 3]. Shaking a box of beads, no matter how hard, fails to generate a thermal distribution of energy. Instead, the velocity distributions are not Maxwellian [4, 5, 6] and energy may be distributed unevenly in space [7, 8, 9] or among different components of a polydisperse granular media [10, 11]. Moreover, spatial correlations may spontaneously develop [12]. Granular gases also exhibit interesting collective phenomena such as shocks [13, 14], clustering [15, 16, 17, 18, 19], and hydrodynamic instabilities [20, 21]. Energy dissipation, which results from inelastic collisions, is largely responsible for this rich phenomenology.

Dilute granular matter can be studied systematically using kinetic theory. This approach has been used to quantitatively model situations where the dynamics are primarily collisional [22, 23, 24, 25]. Kinetic theory has been used to derive transport coefficients in the continuum theory of rapid granular flows, and it has also been used to model freely evolving and driven granular gases.

Spatially homogeneous systems are a natural starting point for investigations of granular gases. Theoretical, computational, and experimental studies show that the system cools indefinitely without energy injection, and that it reaches a steady-state when energy is injected to counter the dissipation. In the freely cooling case, the velocity distribution follows a self-similar form and in the forced case, the velocity distribution approaches a steady-state. In either case, the velocity distributions have sharp tails, and in particular, all of their moments are finite.

In this study, we consider the very same spatially ho-

mogeneous granular gases and show that there is an additional family of steady and transient states. First, we demonstrate that for a special, analytically soluble case, the unforced Boltzmann equation admits non-trivial stationary states where the velocity distribution has a power-law high-energy tail. Then, we show that in general, the tail of the distribution obeys a linear equation and use this master equation to demonstrate that stationary states with power-law tails are generic, existing for arbitrary dimension and arbitrary collision rules. The characteristic exponents are obtained analytically [26].

The mechanism responsible for these stationary states is an energy cascade from large velocity scales to small velocity scales that occurs due to the inelastic particle collisions. Driven steady-states with the same characteristic exponent and a high velocity cut-off can be maintained by injecting energy at a large velocity scale to compensate for the energy dissipated in the cascade. We confirm these steady-states using Monte Carlo simulations. We propose that such steady states can be experimentally realized in driven granular systems in which energy is injected at large velocities.

There is also a family of closely related freely cooling time-dependent states. We demonstrate this explicitly in one-dimension. In these transient states, the velocity distribution coincides with the stationary distribution up to some large velocity scale, but falls off exponentially beyond that scale. This cut-off velocity obeys Haff's cooling law and decreases algebraically with time until the power-law range collapses. The velocity distribution is self-similar and the underlying scaling function is obtained analytically using the linear Boltzmann equation. These freely cooling states are confirmed using numerical integration of the Boltzmann equation.

This paper is organized as follows. The system is set-up in section II and a special case is solved in section III. Dynamics of large velocities and the linear Boltzmann equation are described in section IV. Stationary states are detailed in section V, driven steady-states in section

\*Electronic address: ebn@lanl.gov

†Electronic address: benjamin.machta@brown.edu

‡Electronic address: machta@physics.umass.edu

VI and transient states in section VII. We conclude in section VIII.

## II. INELASTIC GASES

We study a spatially homogeneous system of identical particles undergoing inelastic collisions. First, we consider one-dimension where the linear collision rule is

$$v_{1,2} = pu_{1,2} + qu_{2,1} \quad (1)$$

with  $v_{1,2}$  the post collision velocity and  $u_{1,2}$  the pre-collision velocity. The collision parameters  $p$  and  $q$  obey  $p + q = 1$ . The relative velocity is reduced by the restitution coefficient  $r = 1 - 2p$  as follows:  $(v_1 - v_2) = -r(u_1 - u_2)$ . In each collision, momentum is conserved, but the total kinetic energy decreases. The energy loss is  $\Delta E = pq(u_1 - u_2)^2$ . Energy dissipation is maximal for the extreme case of completely inelastic collisions ( $r = 0, p = 1/2$ ) and it vanishes for the extreme case of elastic collisions ( $r = 1, p = 0$ ).

In this study, we consider the general collision rate

$$K(u_1, u_2) = |u_1 - u_2|^\lambda \quad (2)$$

with  $0 \leq \lambda \leq 1$  the homogeneity index. For particles interacting via the central potential  $U(r) \sim r^{-\nu}$ , the homogeneity index is  $\lambda = 1 - 2\frac{d-1}{\nu}$  [27, 28]. There are two limiting cases: (i) Hard-spheres, where the collision rate is linear in the velocity difference,  $\lambda = 1$ , are used to model ordinary granular media; (ii) Maxwell-molecules, where the collision rate is independent of the velocity are used to model granular media with certain dipole interactions [29, 30, 31, 32, 33].

Let  $f(v, t)$  be the distribution of particles with velocity  $v$  at time  $t$ . It is normalized to unity,  $\int dv f(v) = 1$  (henceforth the dependence on  $t$  is left implicit). For freely evolving and spatially homogeneous systems the distribution obeys the Boltzmann equation

$$\begin{aligned} \frac{\partial f(v)}{\partial t} = & \iint du_1 du_2 |u_1 - u_2|^\lambda f(u_1) f(u_2) \\ & \times \left[ \delta(v - pu_1 - qu_2) - \delta(v - u_1) \right]. \end{aligned} \quad (3)$$

In this master equation, the kernel equals the collision rate (2) and the gain and loss terms simply reflect the collision law (1). The Boltzmann equation assumes perfect mixing as the probability of finding two particles at the same position is taken as proportional to the product of the individual particle probabilities. It is exact when the strong condition of perfect mixing or “molecular chaos” is met, but it is only approximate when the particle positions are correlated.

One well-known solution of the this equation is the “homogeneous cooling state” where the velocity distribution is self-similar in the long time limit [34, 35],

$$f(v, t) \simeq \frac{1}{v_0} \psi\left(\frac{v}{v_0}\right) \quad (4)$$

with the characteristic velocity  $v_0$ . Applying dimensional analysis, the collision rate  $K \propto v_0^\lambda$  should be inversely proportional to time,  $K \sim t^{-1}$ . This leads to Haff’s cooling law [38]

$$v_0 \sim t^{-1/\lambda}. \quad (5)$$

Alternatively, it follows from the rate equation  $dv_0/dt \propto -v_0^{1+\lambda}$ , implying that exponential decay occurs for the limiting case of Maxwell molecules. Statistics of energetic particles are characterized by the tail of the distribution, and for freely cooling states, there is a stretched exponential decay [34, 36, 37]

$$\psi(z) \sim \exp(-|z|^\lambda), \quad (6)$$

for  $\lambda > 0$  as  $|z| \rightarrow \infty$ .

In the freely cooling states, all energy is dissipated from the system and the particles come to rest,  $f(v, t) \rightarrow \delta(v)$  as  $t \rightarrow \infty$ . Thus, the system reaches a trivial stationary state. Are there any nontrivial stationary states? Quite surprisingly, the answer is yes. Our main result is that generically, there is a family of nontrivial stationary solutions of the Boltzmann equation.

## III. AN EXACT SOLUTION

The stationary velocity distribution can be obtained analytically for one-dimensional Maxwell molecules. Since the governing equation (3) is in a convolution form, it is natural to employ the Fourier transform [39],  $F(k) = \int dv e^{ikv} f(v)$ . The stationary state ( $\partial/\partial t \equiv 0$ ) satisfies the non-local and non-linear equation [40, 41]

$$F(k) = F(pk)F(qk). \quad (7)$$

Normalization implies  $F(0) = 1$ .

For elastic collisions,  $p = 0$ , every distribution is a stationary state, but this is a one-dimensional anomaly, because in higher dimensions, the stationary distribution is always Maxwellian [29]. For all  $0 \leq p \leq 1$  and  $p+q = 1$ , there is a family of stationary solutions

$$F(k) = \exp(-v_0|k|), \quad (8)$$

characterized by the arbitrary typical velocity  $v_0$ . Performing the inverse Fourier transform, the velocity distribution is a Lorentz (Cauchy) distribution [42]

$$f(v) = \frac{1}{\pi v_0} \frac{1}{1 + (v/v_0)^2}. \quad (9)$$

This distribution decays algebraically at large velocities. For freely cooling Maxwell-molecules in one-dimension, the velocity distribution has a related form, a squared Lorentzian [43].

This stationary distribution does not evolve under the collision dynamics since at each velocity there is perfect balance between collisional loss and collisional gain. The total energy density and the total dissipation rate are both divergent due to the shallow tail of the velocity distribution.

#### IV. CASCADE DYNAMICS

To analyze the general behavior, we focus on the dynamics of very energetic particles. This allows us to derive the power-law decay and to obtain the characteristic exponent for all spatial dimensions and all collision parameters.

##### A. One-Dimension

The collision integral in Eq. (3) greatly simplifies in the limit  $v \rightarrow \infty$ . Since the distribution decays sharply at large velocities, the product  $f(u_1)f(u_2)$  is maximal when one of the pre-collision velocities is large and the other small. For the gain term there are two possibilities: either  $u_1 \gg u_2$  and then  $v = pu_1$  or  $u_2 \gg u_1$  and then  $v = qu_2$ . Let us denote the large velocity by  $u$  and the small one by  $w$ . The double integral separates into two independent integrals,

$$\frac{\partial f(v)}{\partial t} = \int dw f(w) \int du |u|^\lambda f(u) \times [\delta(v - pu) + \delta(v - qu) - \delta(u)]. \quad (10)$$

Here, the collision rate  $|u - w|^\lambda$  was approximated by  $|u|^\lambda$ . The integral over the smaller velocity equals one, and performing the integration over the larger velocity yields

$$\frac{\partial f(v)}{\partial t} = |v|^\lambda \left[ \frac{1}{p^{1+\lambda}} f\left(\frac{v}{p}\right) + \frac{1}{q^{1+\lambda}} f\left(\frac{v}{q}\right) - f(v) \right]. \quad (11)$$

The tail of the velocity distribution satisfies a non-local but *linear* evolution equation.

The linear Boltzmann equation is valid for broader conditions compared with the full nonlinear Boltzmann equation. The only requirement is that energetic particles are uncorrelated with slower particles. This is a weaker condition than the “*stosszahlansatz*” that the two particle density be equal to a product of one-particle densities.

Eq. (11) reflects that large velocities undergo the following cascade process

$$v \rightarrow (pv, qv), \quad (12)$$

with the rate  $|v|^\lambda$ . These cascade dynamics follow directly from the collision rule (1) by setting one of the incoming velocities to zero. Even though the number of particles is conserved, the number of energetic particles doubles in each cascade event (Fig. 1). Moreover, momentum is conserved but energy is dissipated in each cascade event: it is transferred from large velocities to smaller velocities.

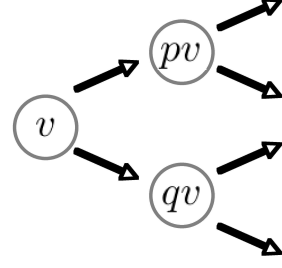


FIG. 1: The cascade process.

##### B. Arbitrary Dimension

In general dimensions, the collision rule is

$$\mathbf{v}_1 = \mathbf{u}_1 - (1 - p)(\mathbf{u}_1 - \mathbf{u}_2) \cdot \hat{\mathbf{n}} \hat{\mathbf{n}}. \quad (13)$$

Here  $\hat{\mathbf{n}} \equiv \mathbf{n}/n$  with  $n \equiv |\mathbf{n}|$  is a unit vector parallel to the impact direction  $\mathbf{n}$  (connecting the particle centers),  $\mathbf{v}_{1,2}$  are the post-collision velocities, and  $\mathbf{u}_{1,2}$  are the pre-collision velocities. The normal (to  $\hat{\mathbf{n}}$ ) component of the relative velocity is reduced by the restitution coefficient  $r = 1 - 2p$  as follows,  $(\mathbf{v}_1 - \mathbf{v}_2) \cdot \hat{\mathbf{n}} = -r(\mathbf{u}_1 - \mathbf{u}_2) \cdot \hat{\mathbf{n}}$  and the energy dissipated equals  $p(1 - p)|(\mathbf{u}_1 - \mathbf{u}_2) \cdot \hat{\mathbf{n}}|^2$ . Similarly, the general collision rate (2) becomes  $K(\mathbf{u}_1, \mathbf{u}_2) = |(\mathbf{u}_1 - \mathbf{u}_2) \cdot \hat{\mathbf{n}}|^\lambda$ . The velocity distribution  $f_d(\mathbf{v})$  satisfies

$$\frac{\partial}{\partial t} f_d(\mathbf{v}) = \iiint d\hat{\mathbf{n}} d\mathbf{u}_1 d\mathbf{u}_2 |(\mathbf{u}_1 - \mathbf{u}_2) \cdot \hat{\mathbf{n}}|^\lambda f_d(\mathbf{u}_1) f_d(\mathbf{u}_2) \times [\delta(\mathbf{v} - \mathbf{v}_1) - \delta(\mathbf{v} - \mathbf{u}_1)]. \quad (14)$$

In addition to integration over the incoming velocities, an additional integration over the impact direction is required, and this integration is normalized,  $\int d\hat{\mathbf{n}} = 1$ . The impact angle is assumed to be uniformly distributed.

The dynamics of large velocities  $v \rightarrow \infty$  are simplified as in the one-dimensional case. The integration over the incoming velocities is separated into an integral over a small velocity and an integral over a large velocity  $\mathbf{u}$ . The former integration is immediate,

$$\frac{\partial}{\partial t} f_d(\mathbf{v}) = \iint d\hat{\mathbf{n}} d\mathbf{u} |\mathbf{u} \cdot \hat{\mathbf{n}}|^\lambda f_d(\mathbf{u}) \times [\delta(\mathbf{v} - (1 - p)\mathbf{u} \cdot \hat{\mathbf{n}} \hat{\mathbf{n}}) + \delta(\mathbf{v} - \mathbf{u} + (1 - p)\mathbf{u} \cdot \hat{\mathbf{n}} \hat{\mathbf{n}}) + \delta(\mathbf{v} - \mathbf{u})]. \quad (15)$$

Let  $\mu = (\hat{\mathbf{u}} \cdot \hat{\mathbf{n}})^2$ ; in other words, if  $\theta$  is the angle between the dominant velocity and the impact angle, then  $\mu = \cos^2 \theta$ . There are two gain terms corresponding to the two cases  $\mathbf{v} = (1 - p)\mathbf{u} \cdot \hat{\mathbf{n}} \hat{\mathbf{n}}$  and  $\mathbf{v} = \mathbf{u} - (1 - p)\mathbf{u} \cdot \hat{\mathbf{n}} \hat{\mathbf{n}}$ . These collision rules, together with the impact angle, dictate the magnitudes of the post-collision velocity in terms of the pre-collision velocity,  $v = \alpha u$  and  $v = \beta u$  with the following stretching parameters

$$\alpha = (1 - p)\mu^{1/2}, \quad (16a)$$

$$\beta = [1 - (1 - p^2)\mu]^{1/2}. \quad (16b)$$

The parameter  $\alpha$  follows from  $\hat{\mathbf{u}} = \hat{\mathbf{n}}$  and the parameter  $\beta$  is obtained by introducing  $\mathbf{w} = \mathbf{v} - \mathbf{u}$  and then employing the collision rule  $w = -\mathbf{w} \cdot \hat{\mathbf{n}} = (1-p)\mathbf{u} \cdot \hat{\mathbf{n}} = (1-p)u\mu^{1/2}$  and the identity  $v^2 = u^2 + w^2 - 2uw\mu^{1/2}$ . The integration over the large velocity  $\mathbf{u}$  includes separate integrations over the velocity magnitude  $u$  and over the velocity direction  $\hat{\mathbf{u}}$  but since this angle is a unique function of the impact angle, the latter integration is immediate. Using the isotropic velocity distribution  $f_d(\mathbf{v}) \equiv S_d v^{d-1} f(v)$  with  $S_d \int dv v^{d-1} f(v) = 1$  and  $S_d$  the area of the  $d$ -dimensional unit hypersphere, Eq. (15) simplifies to

$$v^{d-1} \frac{\partial f(v)}{\partial t} = \iint d\hat{\mathbf{n}} du |u\mu^{1/2}|^\lambda u^{d-1} f(u) \times [\delta(v - \alpha u) + \delta(v - \beta u) - \delta(v - u)]. \quad (17)$$

Finally, we simplify the angular integration,  $d\hat{\mathbf{n}} \propto \sin^{d-2} \theta d\theta$ . Denoting the angular integration with angular brackets  $\langle g \rangle \equiv \int d\hat{\mathbf{n}} g(\hat{\mathbf{n}})$ , we have

$$\langle g \rangle = C \int_0^1 d\mu g(\mu) \mu^{-1/2} (1 - \mu)^{\frac{d-3}{2}}. \quad (18)$$

The constant  $C = 1/B(\frac{1}{2}, \frac{d-1}{2})$ , with  $B(a, b)$  the beta function, is set by normalization. The linear equation governing the tail of the distribution is therefore

$$\frac{\partial f(v)}{\partial t} = \left\langle v^\lambda \mu^{\lambda/2} \left( \frac{1}{\alpha^{d+\lambda}} f\left(\frac{v}{\alpha}\right) + \frac{1}{\beta^{d+\lambda}} f\left(\frac{v}{\beta}\right) - f(v) \right) \right\rangle. \quad (19)$$

As in one-dimension, large velocities undergo the cascade process

$$v \rightarrow (\alpha v, \beta v), \quad (20)$$

but in general dimension, the stretching parameters acquire a dependence on the impact angle. In each collision, the total velocity magnitude increases, despite the fact that the total energy decreases, as reflected by the following two inequalities

$$\alpha + \beta \geq 1, \quad (21a)$$

$$\alpha^2 + \beta^2 \leq 1. \quad (21b)$$

Equalities occur in the limiting cases: the total velocity magnitude is conserved in one dimension where collisions are always head-on ( $\mu = 1$ ) and, of course, the total energy is conserved for elastic collisions ( $p = 0$ ). Actually, a stronger statement than (21) holds: the quantity  $M_s(\alpha, \beta) = \alpha^s + \beta^s - 1$  is positive for  $s \leq 1$ , negative for  $s \geq 2$ , and it may be either positive or negative in the range  $1 < s < 2$ , depending on the impact angle.

## V. STATIONARY STATES

We have seen that the velocity distribution decays algebraically for one-dimensional Maxwell molecules. The

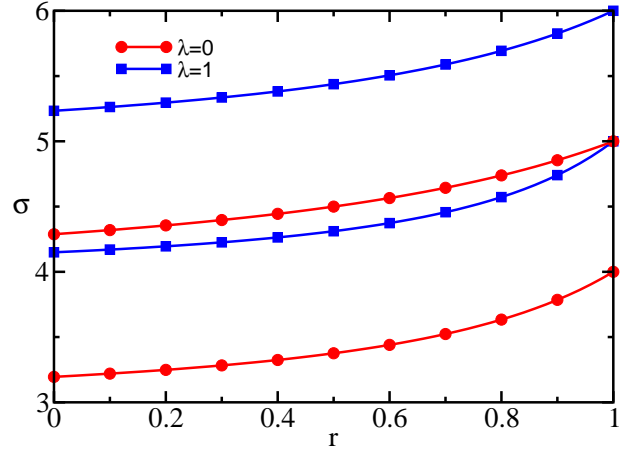


FIG. 2: The exponent  $\sigma$  versus the restitution coefficient  $r$  for hard-spheres ( $\lambda = 1$ ) and Maxwell molecules ( $\lambda = 0$ ). The top two curves are for  $d = 3$  and the bottom two curves are for  $d = 2$ .

linear equation for the tail of the distribution shows that this behavior extends to all  $\lambda$  and all  $p$  in one-dimension. The power-law velocity distribution

$$f(v) \sim v^{-\sigma} \quad (22)$$

satisfies the linear Boltzmann equation (11) with the time derivative set to zero when  $p^{\sigma-1-\lambda} + q^{\sigma-\lambda-1} = 1$ . Since the collision parameters satisfy  $p + q = 1$ , the characteristic exponent in one-dimension is simply

$$\sigma = 2 + \lambda. \quad (23)$$

Of course, the power-law behavior applies only for the tail of the distribution.

Algebraic behavior holds in arbitrary dimension. Substituting Eq. (22) into the general linear Boltzmann equation (19), the characteristic exponent is root of the equation

$$\left\langle (\alpha^{\sigma-d-\lambda} + \beta^{\sigma-d-\lambda} - 1) \mu^{\lambda/2} \right\rangle = 0. \quad (24)$$

This transcendental equation can be re-written explicitly in terms of the gamma function and the hypergeometric function [44]

$$\frac{1 - {}_2F_1\left(\frac{d+\lambda-\sigma}{2}, \frac{\lambda+1}{2}, \frac{d+\lambda}{2}, 1-p^2\right)}{(1-p)^{\sigma-d-\lambda}} = \frac{\Gamma(\frac{\sigma-d+1}{2})\Gamma(\frac{d+\lambda}{2})}{\Gamma(\frac{\sigma}{2})\Gamma(\frac{\lambda+1}{2})}. \quad (25)$$

The exponent  $\sigma \equiv \sigma(d, \lambda, r)$  varies continuously with the spatial dimension  $d$ , the homogeneity index  $\lambda$ , and the restitution coefficient  $r$  (figure 2).

According to the bounds (21) the left hand side of Eq. (24) is positive when  $\sigma - d - \lambda \leq 1$  but negative when  $\sigma - d - \lambda \geq 2$ . Therefore, this quantity changes sign when  $1 \leq \sigma - d - \lambda \leq 2$  leading to the relatively tight bounds

$$d + 1 + \lambda \leq \sigma \leq d + 2 + \lambda. \quad (26)$$

The lower bound (23) is realized in one-dimension where the collisions are always head-on, while the upper bound is approached,  $\sigma \rightarrow d + 2 + \lambda$ , in the quasi-elastic limit  $r \rightarrow 1$ . We note that the two limiting cases of one-dimension and elastic collisions do not commute. Moreover, the zero dissipation limit is singular: Maxwellian distributions occur when the collisions are elastic [29].

Since the energy lost in each collision is proportional to  $(\Delta v)^2$  and the collision rate is proportional to  $|\Delta v|^\lambda$ , the energy dissipation rate is related to the following integral,  $\Gamma \sim \langle v^{2+\lambda} \rangle$  where  $\langle g(v) \rangle \equiv S_d \int dv v^{d-1} f(v) g(v)$ . Hence, the bound  $\sigma \leq d + 2 + \lambda$  implies that the total dissipation rate is divergent. This is a generic feature of the stationary solutions, and in fact it shows why Haff's cooling law  $dT/dt = -\Gamma$ , where  $T = \langle v^2 \rangle$  is the granular temperature, does not apply: this rate equation assumes finite dissipation rates. In contrast, the total energy may be either finite or infinite because both  $\sigma > d + 2$  and  $\sigma < d + 2$  are possible. The stationary states studied here appear to be fundamentally different than the infinite energy solutions of the elastic Boltzmann equation because they require dissipation and because they always involve infinite dissipation [45].

The characteristic exponent increases monotonically with the spatial dimension, the homogeneity index, and the restitution coefficient. Thus, fixing  $d$  and  $\lambda$ , the completely inelastic case ( $r = 0$ ) provides a lower bound for  $\sigma$  with respect to  $r$  (figure 2). For hard-spheres the completely inelastic limit yields  $\sigma = 4.1922$  and  $\sigma = 5.23365$  in two- and three-dimensions, while for Maxwell molecules the corresponding values are  $\sigma = 3.19520$  and  $\sigma = 4.28807$ .

The power-law behavior is in sharp contrast with the stretched exponential tails  $f(v) \sim \exp(-|v|^\delta)$  that typically characterize granular gases. For freely cooling gases,  $\delta = \lambda$  as in (6), and for thermally forced gases,  $\delta = 1 + \lambda/2$  [46, 47, 48, 49]. Both behaviors immediately follow from the linear Boltzmann equation (19); in the forced case, the time derivative in (19) is replaced by the diffusive forcing term  $\partial/\partial t \rightarrow D\nabla^2$ . Only in the limiting case of freely cooling Maxwell molecules do power-law velocity distributions arise, but the solutions are not stationary and the characteristic exponent differs from the stationary solutions [50, 51, 52, 53].

## VI. DRIVEN STEADY-STATES

In this section we describe driven, non-equilibrium steady-states that are identical, except for a high velocity cut-off, to the stationary states described above. In these steady-states energy is injected at a large velocity scale, cascades to small velocities, and is dissipated over a broad power-law range. The energy injection scale  $V$  must be well separated from the typical velocity scale  $v_0$ , but otherwise, the injection mechanism is not unique. We study several concrete cases where energy is injected with a small rate at a large velocity.

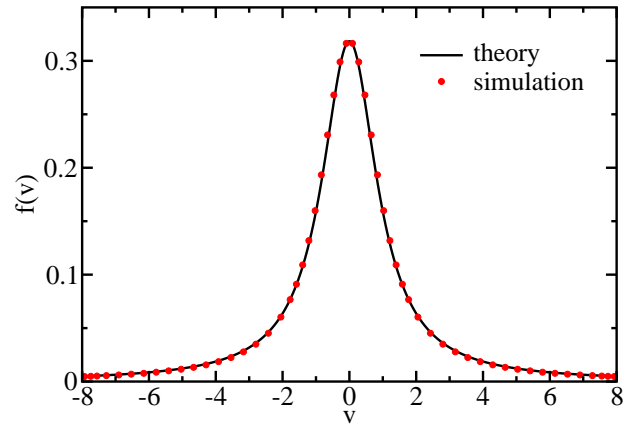


FIG. 3: The velocity distribution for one-dimensional Maxwell molecules. The solid line is a Lorentzian and the typical velocity is  $v_0 = 0.055$ .

As we have seen in the exactly soluble case of one-dimensional Maxwell molecules, there is a family of steady-state solutions characterized by the typical velocity  $v_0$ : if  $f(v)$  is a steady-state solution, so is  $v_0^{-d} f(v/v_0)$  for arbitrary  $v_0$ . Let the energy injection rate (per particle) be  $\gamma$  and let the injection velocity be  $V$ . This scale sets an upper cutoff on the velocity distribution, beyond which the distribution should rapidly vanish. Since the system is at a steady-state, the dissipation rate

$$\begin{aligned} \Gamma &\sim \langle v^{2+\lambda} \rangle \sim \int^V dv v^{d+1+\lambda} v_0^{-d} f(v/v_0) \\ &\sim V^{\lambda+2} (V/v_0)^{d-\sigma}, \end{aligned} \quad (27)$$

must be balanced by the energy injection rate  $\gamma V^2$ , leading to a general relation between the injection rate, the injection velocity and the typical velocity,

$$\gamma \sim V^\lambda (V/v_0)^{d-\sigma}. \quad (28)$$

To verify the theoretical predictions, we performed Monte Carlo simulations. Collisions are simulated by selecting two particles at random with a probability proportional to the collision rate and then updating their velocities according to the collision rule (13). Energy is injected with a small rate using the following “lottery” implementation. An energy loss counter keeps track of the cumulative energy loss. With a small rate, a randomly chosen particle is “awarded” an energy equal to the reading on the loss counter. Subsequently, the loss counter is reset to zero. With this protocol, the kinetic energy remains practically constant, and moreover, energy injection occurs only at large velocity scales. For one-dimensional hard-spheres, we tested a different injection mechanism. The injection energy was drawn from a Maxwell-Boltzmann distribution with a very large energy. With a small rate, this energy was added to a randomly chosen particle.

We simulated completely inelastic Maxwell molecules and hard spheres in one- and two-dimensions starting

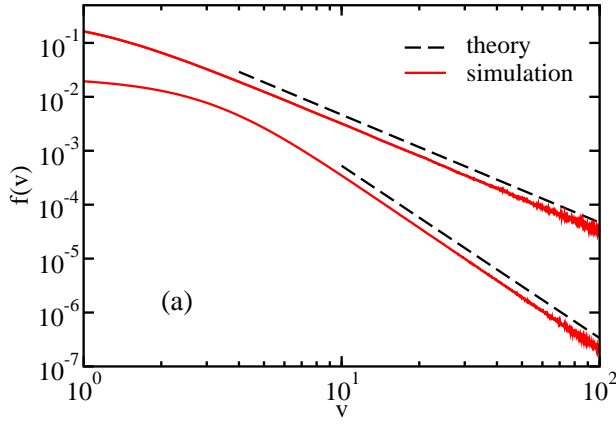


FIG. 4: The velocity distribution for Maxwell molecules. The top curves correspond to one-dimension and the bottom curves to two-dimensions.

with a uniform velocity distribution with support in the range  $[-1 : 1]$ . After a short transient, the system reaches a steady-state. For the special case of one-dimensional Maxwell molecules, we verified that the velocity distribution is Lorentzian (figure 3). In all cases, the tail of the velocity distribution decays as a power-law, and the exponent  $\sigma$  is in excellent agreement with the theoretical prediction, Eq. (25). Maxwell molecule simulation results are displayed in figure 4 and hard sphere simulation results in figure 5.

The energy balance relation (28), combined with the constant energy condition  $\langle v^2 \rangle \sim 1$ , imposed in our simulations, yields an estimate for the typical velocity. Different behaviors emerge for finite energy and infinite energy distributions.

When  $\sigma < d+2$ , the constant energy constraint implies  $V^{d+2-\sigma} \sim v_0^{d-\sigma}$ , that combined with energy balance (28) reveals how the maximal velocity and the typical velocity scale with the injection rate

$$V \sim \gamma^{-\frac{1}{2-\lambda}}, \quad (29a)$$

$$v_0 \sim \gamma^{\frac{d+2-\sigma}{(\sigma-d)(2-\lambda)}}. \quad (29b)$$

Simulations with  $d = 1$ ,  $\lambda = 0$ , and  $\gamma = 10^{-4}$ , are characterized by  $V \approx 10^2$  and  $v_0 \approx 10^{-2}$ , consistent with these scaling laws.

In the complementary case,  $\sigma > d+2$ , the typical velocity  $v_0 \sim 1$  is set by the initial conditions because  $\langle v^2 \rangle \sim v_0^2$ . Energy balance (28) yields

$$V \sim \gamma^{-\frac{1}{\sigma-d-\lambda}}. \quad (30)$$

Simulations with  $d = 2$ ,  $\lambda = 1$ , and  $\gamma = 10^{-2}$  should be characterized by the injection scale  $V \approx 50$ , as in this case  $\sigma \cong 4.15$ . The data is consistent with this estimate.

As long as the system is sufficiently large, there is no dependence on the system size (the number of particles). The total energy and the total dissipation rate are proportional to the system size, and in general, all thermodynamic properties are extensive.

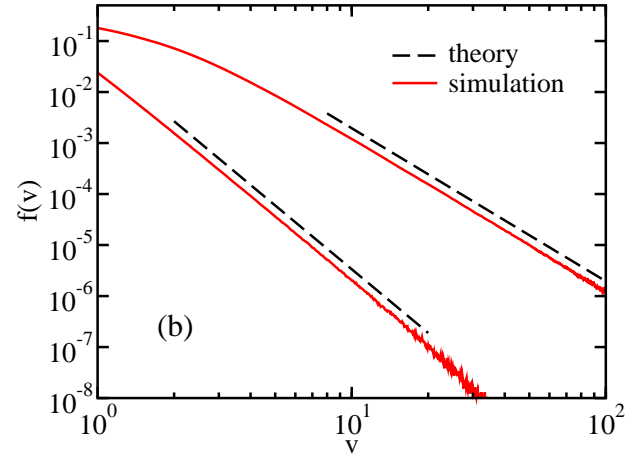


FIG. 5: The velocity distribution for hard spheres in one-dimension (top curves) and in two-dimensions (bottom curves).

Based on the theoretical and the simulation results, we conclude that there may be qualitative differences between the finite energy and infinite energy cases, but that fundamentally, the steady-state solutions are of one nature. They represent a nonequilibrium stationary-state where energy is injected at velocity scale  $V$  and dissipated at velocity scale  $v_0$ . These scales are set by the injection rate and the injection protocol.

## VII. TIME-DEPENDENT STATES

What happens to these steady states when energy injection is turned-off? Steady-state solutions of the type (22) can be realized only up to some upper cutoff. Such truncated power-law distributions are still compact, and thus, in the absence of energy input, they should undergo free cooling with all energy eventually dissipated from the system.

Therefore, we anticipate that there is a time-dependent velocity cut-off  $V(t)$ . Below this scale the distribution is nearly the same as the stationary distribution but above this scale, the distribution has a sharp tail, analogous to the freely cooling state (4). Thus, the distribution is of the form  $f(v, t) \equiv f(v, V)$  such that for  $v < V(t)$ ,  $f(v; V) \approx f_s(v)$  while for  $v > V(t)$ , the distribution decays faster than a power law. Here  $f_s(v)$  is the stationary solution of the full Boltzmann equation. We assume that the cut-off scale is much larger than the typical velocity,  $V \gg v_0$  and, without loss of generality, set  $v_0 \equiv 1$ . The assumption that the distribution is unmodified below the cut-off velocity is consistent with the character of the energy cascade. Furthermore, we expect that the functional form of the cut-off depends only on the scaled variable,  $v/V$ .

First, consider the time dependence of the cut-off scale  $V(t)$ . Given the assumption that cooling occurs only

through a decrease in the cut-off scale, the rate of change of the energy is

$$\begin{aligned} \frac{dE}{dt} &= \frac{d\langle v^2 \rangle}{dt} = \frac{d}{dt} \int^{V(t)} dv v^{d+1} f_s(v) \\ &\sim V^{d+1-\sigma} \frac{dV}{dt}. \end{aligned} \quad (31)$$

The decrease in energy equals the dissipation rate  $\Gamma \sim V^{d+2+\lambda-\sigma}$  from Eq. (27), showing that the cut-off velocity obeys Haff's cooling law,

$$\frac{dV}{dt} = -cV^{1+\lambda}. \quad (32)$$

Therefore, the cut-off velocity decays with time as follows

$$V(t) = \left[ \frac{V^\lambda(0)}{1 + c\lambda V^\lambda(0)t} \right]^{1/\lambda} \quad (33)$$

where  $V(0)$  is the initial value of the cut-off.

Restricting our attention to one-dimension we seek similarity solutions of the type

$$f(v, t) \simeq f_s(v) \phi\left(\frac{v}{V}\right). \quad (34)$$

Here,  $f_s(v)$  is the stationary solution of Eq. (3) that decays as a power-law at large velocities  $f_s(v) \simeq Av^{-2-\lambda}$ . The cut-off function approaches unity at small arguments,  $\phi(x) \rightarrow 1$  as  $x \rightarrow 0$  so that the stationary solution is recovered for  $v \ll V$ .

Substituting the time dependent form (34) into the linear governing equation (11) yields

$$-\frac{dV/dt}{V^{1+\lambda}} \phi'(x) = x^{\lambda-1} \left[ p\phi\left(\frac{x}{p}\right) + q\phi\left(\frac{x}{q}\right) - \phi(x) \right]. \quad (35)$$

Assuming the cut-off velocity satisfies Eq. (32) with constant of proportionality  $c$ , the scaling function satisfies the linear and non-local differential equation

$$c\phi'(x) = x^{\lambda-1} \left[ p\phi\left(\frac{x}{p}\right) + q\phi\left(\frac{x}{q}\right) - \phi(x) \right], \quad (36)$$

with the boundary conditions  $\phi(0) = 1$  and  $\phi(x) \rightarrow 0$  as  $x \rightarrow \infty$ . Note that  $\phi(x)$  must be non-analytic at  $x = 0$  because all its derivatives vanish at  $x = 0$  since  $p + q = 1$  and  $\phi(0) = 1$ .

For large arguments, the last term on the right hand side dominates, and therefore, the tail of the distribution is a stretched exponential as in (6)

$$\phi(x) \sim \exp(-Cx^\lambda) \quad (37)$$

with  $C = (\lambda c)^{-1}$  for  $\lambda > 0$ . In the limiting case  $\lambda = 0$  all terms on the left-hand side are comparable and the tail is algebraic:  $\phi(x) \sim x^{-\sigma}$  with  $c\sigma = 1 - p^{\sigma+1} - q^{\sigma+1}$ . Thus, both the decay of the cut-off velocity and the tail behavior are as for ordinary freely cooling solutions,

Eq. (4). There is, however, a difference since the distributions considered here have *two* characteristic velocities,  $V$  and  $v_0$  and it is only the upper cut-off,  $V$  that evolves in time. After  $V$  and  $v_0$  become comparable, the behavior crosses over to the homogeneous cooling state [34, 35] with a single characteristic velocity,  $v_0$ .

We now focus on completely inelastic hard-spheres ( $\lambda = 1$  and  $p = q = 1/2$ ) for which an exact solution is possible. Integrating Eq. (36) and imposing  $\phi(0) = 1$  gives  $c = (1 - p^2 - q^2) \int_0^\infty dx \phi(x)$ , but since the cut-off scale  $V$  is defined up to a constant, we may set the integral value,  $\int_0^\infty dx \phi(x) = 1$  leading to  $c = 1 - p^2 - q^2$ . When  $p = q = 1/2$  then  $c = 1/2$  and Eq. (36) becomes

$$\phi'(x) = 2[\phi(2x) - \phi(x)]. \quad (38)$$

This equation can be solved using the Laplace transform  $h(s) = \int dx e^{-sx} \phi(x)$ , that satisfies the non-local equation

$$(2 + s)h(s) = 1 + h(s/2) \quad (39)$$

with the boundary condition  $h(0) = 1$  set by the normalization. Since  $\phi(x) \rightarrow 1$  as  $x \rightarrow 0$  then  $h(s) \rightarrow s^{-1}$  as  $s \rightarrow \infty$ , so we make the transformation  $h(s) = s^{-1} [1 - g(s)]$  with  $g(0) = 1$  and  $g'(0) = -1$ . The auxiliary function  $g(s)$  satisfies a recursion-like equation  $g(s) = (1 + s/2)^{-1} g(s/2)$ . Solving iteratively and invoking  $g(0) = 1$ , the solution is the infinite product  $g(s) = \prod_{n=1}^\infty (1 + s/2^n)^{-1}$ , and the Laplace transform is

$$h(s) = \frac{1}{s} \left( 1 - \prod_{n=1}^\infty \frac{1}{1 + \frac{s}{2^n}} \right). \quad (40)$$

Since the infinite product has a series of simple poles at  $s = -2^{-n}$  for every integer  $n \geq 1$ , the scaling function is a sum of exponentials

$$\phi(x) = \sum_{n=1}^\infty a_n \exp(-2^n x) \quad (41a)$$

$$a_n = \prod_{\substack{k=1 \\ k \neq n}}^\infty \frac{1}{1 - 2^{n-k}}, \quad (41b)$$

with the coefficients obtained as the residues to the poles  $a_n = \lim_{s \rightarrow -2^{-n}} [(s + 2^n)h(s)]$ . In contrast with freely cooling states (4), the scaling function  $\phi(x)$  can be obtained exactly.

The Laplace transform conveniently yields the limiting behaviors of the scaling function. The simple pole closest to the origin reflects the tail behavior

$$\phi(x) \simeq a_1 \exp(-2x) \quad (42)$$

as  $x \rightarrow \infty$  with  $a_1 = 3.46275$  obtained from Eq. (41b). More interesting is the small  $x$  behavior, reflected by the large  $s$  behavior

$$\int_0^\infty dx [1 - \phi(x)] e^{-sx} = s^{-1} g(s) \rightarrow s^{-1} \exp[-C(\ln s)^2]$$



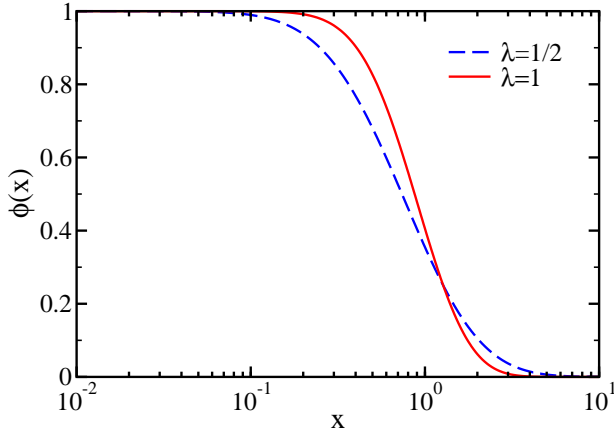


FIG. 6: The scaling function  $\phi(x)$  versus  $x$  for  $\lambda = 1/2$  (dashed line) and  $\lambda = 1$  (solid line).

as  $s \rightarrow \infty$  with  $C = (2 \ln 2)^{-1}$ . The function  $g(s)$  was estimated by replacing the infinite product with a finite product

$$\prod_{n=1}^{\infty} \frac{1}{1 + \frac{s}{2^n}} \cong \prod_{n=1}^{n_*} \frac{2^n}{s} \rightarrow \exp[-C(\ln s)^2] \quad (43)$$

with  $n_* = \ln_2 s$ . Inverting the log-normal Laplace transform using the steepest descent method, the leading correction to the scaling function is log-normal as well

$$1 - \phi(x) \sim \exp \left[ -A \left( \ln \frac{1}{x} \right)^2 \right], \quad (44)$$

as  $x \rightarrow 0$  with  $A = C/4 = (8 \ln 2)^{-1}$ . Thus, the scaling function is perfectly flat near the origin as all its derivatives vanish at  $x = 0$  (figure 6). Physically, the small  $x$  behavior shows that there is a sizable range of velocities for which the time-dependent velocity distribution (34) coincides with the steady-state solution,  $f(v, t) \simeq f_s(v)$ .

The series solution (41) can be straightforwardly generalized to all  $\lambda > 0$

$$\phi(x) = \sum_{n=1}^{\infty} a_n \exp[-(2^n x)^\lambda], \quad (45a)$$

$$a_n = \prod_{\substack{k=1 \\ k \neq n}}^{\infty} \frac{1}{1 - 2^{\lambda(n-k)}}. \quad (45b)$$

Making the transformation  $y = x^\lambda$  and setting the proportionality constant  $c = \lambda^{-1} 2^{-\lambda}$  such that  $c = (1 - 2^{-\lambda}) \int_0^\infty dy \phi(y)$ , Eq. (38) is generalized,  $\phi'(y) = 2^\lambda [\phi(2^\lambda y) - \phi(y)]$ . Consequently, the Laplace transform is obtained from Eq. (40) by replacing  $2^n$  with  $2^{\lambda n}$ , and repeating the steps leading to (41) gives (45). Figure 6 shows the scaling function for  $\lambda = 1/2$ . As  $\lambda$  decreases the cut-off becomes less sharp and the flat region near  $x = 0$  less broad.

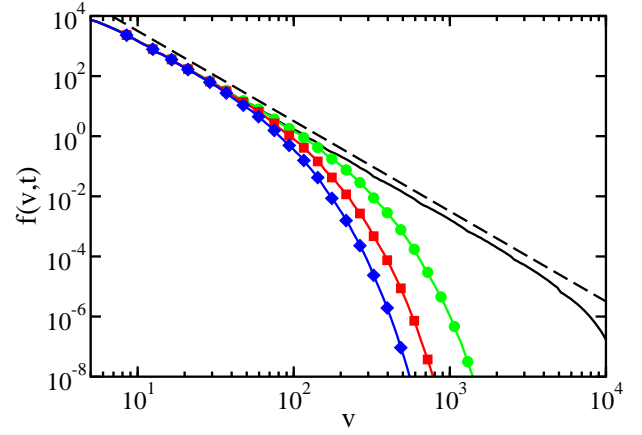


FIG. 7: The velocity distribution  $f(v, t)$  versus  $v$ . Shown is the steady-state distribution before the injection is turned-off (solid line) and at three consecutive and equally-spaced later times (circles, squares, diamonds) during free cooling. Also shown for reference is a dashed line with slope -3. The velocity is in arbitrary units.

In summary, we find that there are time-dependent states associated with the stationary states. In these transient states, the velocity distribution is characterized by a cut-off velocity scale that decays with time according to Haff's law. Below this velocity, the energy cascade is unaffected and the velocity distribution agrees with the stationary distribution but above this scale, the distribution is exponentially suppressed. We relied only on the linear Boltzmann equation to derive a scaling form for the cut-off function. Of course, the full nonlinear equation (3) is still relevant as it governs the dynamics of small velocities via the stationary solution  $f_s(v)$ . This guarantees that the velocity distribution is properly normalized, and specifically, that the integral over small velocities remains finite.

We numerically integrated the hard-sphere Boltzmann equation in one-dimension to verify these predictions. Velocity bins are kept, each with a double precision number representing the number of particles within that velocity range. In the simulation, two velocity bins are chosen randomly with a rate proportional to the collision rate. When two bins "collide", particles are transferred from each into target bins, determined by the collision rule (1).

We generated the stationary distribution by injecting energy at a fixed rate. This was done by uniformly removing particles from the distribution and re-injecting them according to a Gaussian distribution with a large characteristic velocity. Once the system reaches the stationary state, we turn off the energy injection and observe the distribution  $f(v, t)$  as it cools.

Figure 7 shows the driven steady-state distribution and the freely cooling distributions at three later times. The results verify that the steady-state has a power-law tail,  $f_s(v) \sim v^{-3}$  and that the freely cooling distributions are close to the steady-state distribution for sufficiently



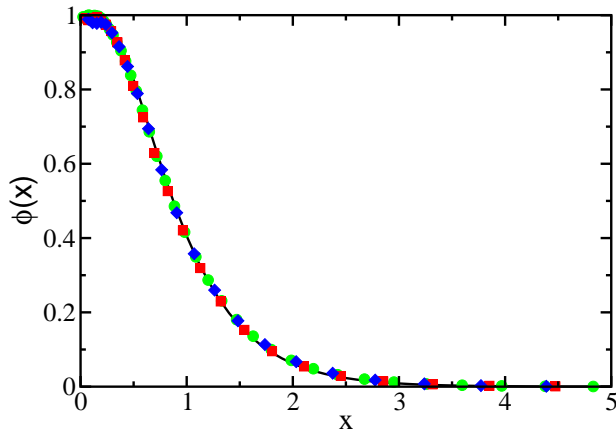


FIG. 8: The scaling function underlying the velocity distribution. The velocity distributions in figure 7 were normalized by the stationary distribution as in Eq. (34). The solid line is the theoretical scaling function (41).

small velocities. Figure 8 shows the same three time-dependent distributions divided by the steady distribution as in Eq. (34) and rescaled by the cut-off velocity  $V(t)$  to collapse the data onto the theoretical prediction (41).

The time dependence of the cut-off velocity, given by Eq. (32), holds until  $V$  is order  $v_0 \equiv 1$ . Thus, the lifetime of the collapsing power-law solution approaches a constant of order unity as  $V(0)$  becomes infinite. During most of the time that the power-law is collapsing,  $V$  decays algebraically with time,  $V(t) \sim t^{-1/\lambda}$ . Figure 9 shows the cut-off velocity versus time together with a fit to the form (33) with  $\lambda = 1$ . We also checked that the tail of the cooling distribution is exponential. We conclude that for completely inelastic hard-spheres, the simulation results are in excellent agreement with the theoretical predictions.

### VIII. CONCLUSIONS

In summary, we find a new class of steady-state and time-dependent states for inelastic gases. In the nonequilibrium steady-states, energy is injected at large velocities, it cascades down to small velocities, and it is dissipated over a power-law range. Generically, the steady-state distributions have a power-law high-energy tail. The characteristic exponents were obtained analytically and they vary with the spatial dimension and the collision rules. Formally, the stationary solutions are characterized by an infinite dissipation rate, while the energy density may be either finite or infinite. In an actual particle system, these steady-states may be realized only up to the energy injection scale, so that all thermodynamic characteristics including the dissipation rate and the energy density are finite.

When injection is turned-off, the velocity distribution

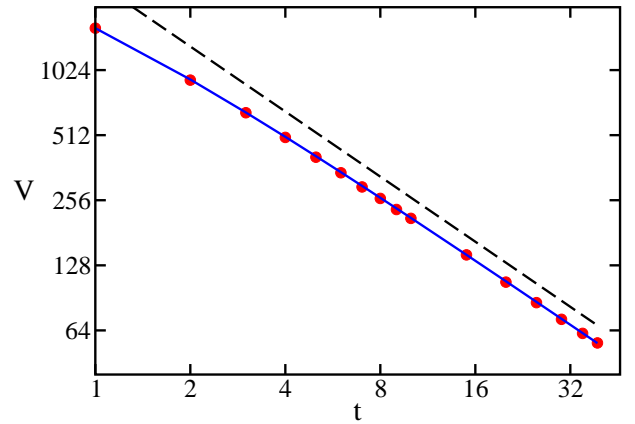


FIG. 9: The cut-off velocity  $V(t)$  as a function of time  $t$  (circles). The solid line is a fit to Eq. (33). Also shown is a broken line with slope  $-1$ .

is stationary only in a shrinking range of velocities and it decays sharply as a stretched exponential at large velocities. For completely inelastic collisions, the scaling function underlying this behavior can be obtained exactly from the linearized Boltzmann equation and at small velocities, there is a subtle log-normal correction to the power-law behavior. Although we analyzed only the one-dimensional case, we expect the same behavior in higher-dimension. These time-dependent states can be loosely thought of as a hybrid between a steady-state solution and the well-known, freely-cooling solution. Both the time-dependence of the characteristic velocity and the decay at large velocities are similar, but not identical, to those occurring for freely cooling granular gases. After the cut-off velocity becomes comparable to the typical velocity, the velocity distribution presumably crosses over to the freely cooling solutions.

Cascade processes occur in many other physical systems. Mathematically, the inelastic cascade process for one-dimensional hard-spheres is identical to that found for the grinding process in Ref. [54], and in both problems  $\sigma = 3$ . Indeed, the cascade process (12) is equivalent to a fragmentation process. In fluid turbulence, the fluid is forced at a large spatial scale, energy cascades from large scales to small scales, where it is dissipated due to viscosity [55]. Actually, the situation found here for granular gases is analogous to wave turbulence, that is described by a kinetic theory for wave collisions [56]. One difference with the Kolmogorov spectra of fluid turbulence is that the characteristic exponents are irrational because they do not follow from dimensional analysis.

Inelastic cascades are a direct consequence of the collision rule and they are described by a linear equation. This equation should be valid under very broad conditions and it can be generalized to nonuniform distributions of impact angles and collision parameters as well as polydisperse granular media. Additionally, the cascade dynamics should extend to viscoelastic collision rules because the restitution coefficient depends only weakly on

the relative velocity for energetic collisions [1].

The most significant condition for these steady-states concerns the driving mechanism: the injection rate must be small compared to the collision rate and the injection energy large compared to the typical energy. We propose that stationary distributions may be achieved in driven granular gas experiments where energy is injected at very large velocity scales. Algebraic tails with exponents comparable with these reported here were observed recently in sheared granular layers, but these experiments involved frictional, rather than collisional, dynamics [57].

Inelastic cascades should also arise when an energetic particle hits a static medium of inelastic particles, or alternatively, a background of slowly moving particles. Indeed, the collision dynamics in this case reduce to the inelastic cascade discussed in this paper. This setup may be interesting to study theoretically and experimentally.

In closing, the kinetic theory of inelastic collisions is remarkable as the nonlinear Boltzmann equation admits a number of distinct solutions including steady-states, transient states, and hybrid states that interpolate between the two. Nonlinearity, nonlocality, and the lack of energy conservation are responsible for this remarkable complexity. We end with an open question: do other families of solutions exist?

### Acknowledgments

We thank P. L. Krapivsky, N. Menon, and V. Zakharov for useful discussions. We acknowledge DOE W-7405-ENG-36, NSF DMR-0242402 and NSF PHY99-07949 for support of this work.

- 
- [1] *Kinetic theory of granular gases*, N. Brilliantov and T. Pöschel, (Oxford, Oxford, 2003).
  - [2] *Granular Gases*, T. Pöschel and S. Luding (editors), (Springer, Berlin, 2000).
  - [3] *Granular Gas Dynamics*, T. Pöschel and N. Brilliantov (editors), (Springer, Berlin, 2003).
  - [4] W. Losert, D. G. W. Cooper, J. Delour, A. Kudrolli, and J. P. Gollub, *Chaos* **9**, 682 (1999).
  - [5] F. Rouyer and N. Menon, *Phys. Rev. Lett.* **85**, 3676 (2000).
  - [6] I. S. Aranson and J. S. Olafsen *Phys. Rev. E* **66**, 061302 (2002).
  - [7] Y. Du, H. Li, and L. P. Kadanoff, *Phys. Rev. Lett.* **74**, 1268 (1995).
  - [8] A. Kudrolli, M. Wolpert and J. P. Gollub, *Phys. Rev. Lett.* **78**, 1383 (1997).
  - [9] E. L. Grossman, T. Zhou, and E. Ben-Naim, *Phys. Rev. E* **55**, 4200 (1997).
  - [10] R. D. Wildman and D. J. Parker, *Phys. Rev. Lett.* **88**, 064301 (2002).
  - [11] K. Feitosa and N. Menon, *Phys. Rev. Lett.* **88**, 198301 (2002).
  - [12] E. Ben-Naim, S. Y. Chen, G. D. Doolen, and S. Redner, *Phys. Rev. Lett.* **83**, 4069 (1999).
  - [13] E. C. Rericha, C. Bizon, M. D. Shattuck, and H. L. Swinney, *Phys. Rev. Lett.* **88**, 014302 (2002).
  - [14] A. Samadani, L. Mahadevan, and A. Kudrolli, *J. Fluid Mech.* **452**, 293 (2002).
  - [15] S. McNamara and W. R. Young, *Phys Fluids A* **4**, 496 (1992).
  - [16] J. S. Olafsen and J. S. Urbach, *Phys. Rev. Lett.* **81**, 4369 (1998).
  - [17] S. Luding and H. J. Herrmann, *Chaos* **9**, 673 (1999).
  - [18] X. Nie, E. Ben-Naim, and S. Y. Chen, *Phys. Rev. Lett.* **89**, 204301 (2002).
  - [19] D. van der Meer, K. van der Weele, and D. Lohse, *Phys. Rev. Lett.* **88**, 174302 (2002).
  - [20] I. Goldhirsch, and G. Zanetti, *Phys. Rev. Lett.* **70**, 1619 (1993).
  - [21] E. Khain and B. Meerson, *Europhys. Lett.* **65**, 193 (2004).
  - [22] J. T. Jenkins and M. W. Richman, *Phys. Fluids* **28**, 3485 (1985).
  - [23] J. J. Brey, J. W. Dufty, C. S. Kim, and A. Santos, *Phys. Rev. E* **58**, 4638 (1998).
  - [24] J. Lutsko, J. J. Brey, and J. W. Dufty, *Phys. Rev. E* **65**, 051304 (2002).
  - [25] I. Goldhirsch, *Ann. Rev. Fluid. Mech.* **35**, 267 (2003).
  - [26] E. Ben-Naim and J. Machta, *Phys. Rev. Lett.* **94**, 138001 (2005).
  - [27] P. Résibois and M. de Leener, *Classical Kinetic Theory of Fluids* (John Wiley, New York, 1977).
  - [28] C. Sire and P. L. Krapivsky, *Phys. Rev. Lett.* **86**, 2494 (2001).
  - [29] J. C. Maxwell, *Phil. Trans. R. Soc.* **157**, 49 (1867).
  - [30] C. Truesdell and R. G. Muncaster, *Fundamentals of Maxwell's Kinetic Theory of a Simple Monoatomic Gas* (Academic Press, New York, 1980).
  - [31] M. H. Ernst, *Phys. Reports* **78**, 1 (1981).
  - [32] A. V. Bobylev, *Sov. Sci. Rev. C. Math. Phys.* **7**, 111 (1988).
  - [33] K. Kohlstedt, A. Snezhko, M. V. Sapozhnikov, I. S. Aranson, J. S. Olafsen, and E. Ben-Naim, preprint (2004).
  - [34] S. E. Esipov and T. Pöschel, *J. Stat. Phys.* **86**, 1385 (1997).
  - [35] J. J. Brey, J. W. Dufty, and A. Santos, *J. Stat. Phys.* **87**, 1051 (1997).
  - [36] M. H. Ernst and R. Brito, *Lecture Notes in Physics* **624**, 1 (2003).
  - [37] A. Barrat, T. Biben, Z. Rácz, E. Trizac, and F. van Wijland, *J. Phys. A* **35**, 463 (2002).
  - [38] P. K. Haff, *J. Fluid Mech.* **134**, 401 (1983).
  - [39] R. S. Krupp, *A nonequilibrium solution of the Fourier transformed Boltzmann equation*, M.S. Thesis, MIT (1967); *Investigation of solutions to the Fourier transformed Boltzmann equation*, Ph.D. Thesis, MIT (1970).
  - [40] E. Ben-Naim and P. L. Krapivsky, *Phys. Rev. E* **61**, R5 (2000).
  - [41] D. ben-Avraham, E. Ben-Naim, K. Lindenberg, and A. Rosas, *Phys. Rev. E* **68**, 031104 (2003).
  - [42] L. Brenig and S. L. Salazar, unpublished.
  - [43] A. Baldassarri, U. M. B. Marconi, and A. Puglisi, *Euro-*

- phys. Lett. **58**, 14 (2002).
- [44] I. S. Gradshteyn and I. M. Ryzhik, *Table of Integrals, Series, and Products*, (Academic Press, New York, 1972).
  - [45] A. V. Bobylev and C. Cercignani, J. Stat. Phys. **106**, 1039 (2002).
  - [46] T. P. C. van Noije and M. H. Ernst, Gran. Matt. **1**, 57 (1998).
  - [47] E. Ben-Naim and P. L. Krapivsky, Lect. Notes. in Phys. **624**, 63 (2003).
  - [48] A. Santos and M. H. Ernst, Phys. Rev. E **68**, 011305 (2003)
  - [49] T. Antal, M. Droz, and A. Lipowski, Phys. Rev. E **66**, 062301 (2002).
  - [50] P. L. Krapivsky and E. Ben-Naim, J. Phys. A **35**, L147 (2002).
  - [51] E. Ben-Naim and P. L. Krapivsky, Phys. Rev. E **66**, 011309 (2002).
  - [52] M. H. Ernst and R. Brito, Europhys. Lett. **58**, 182 (2002).
  - [53] M. H. Ernst and R. Brito, J. Stat. Phys. **109**, 407 (2002).
  - [54] E. Ben-Naim and P.L. Krapivsky Phys. Lett. A **275**, 48 (2000).
  - [55] U. Frisch, *Turbulence: The legacy of A. N. Kolmogorov* (Cambridge University Press, New York, 1995).
  - [56] V. E. Zakharov, V. S. Lvov, and G. Falkovich, *Kolmogorov Spectra of Turbulence I: Wave Turbulence* (Springer-Verlag, New York, 1992).
  - [57] S. Moka and P. R. Nott, cond-mat/0412506.